IUTAM Symposium Wind Waves, 4-8 September 2017, London, UK

Analytic theory of a wind-driven sea

Vladimir Zakharov[a]

[a]University of Arizona, 617 N. Santa Rita Ave., Tucson, AZ 85721-0089 USA

Abstract

A self-sustained analytic theory of a wind-driven sea is presented. It is shown that the wave field can be separated into two ensembles: the Hasselmann sea that consists of long waves with frequency $\omega < \omega_H$, $\omega_H \sim 4 - 5\omega_p$ (ω_p is the frequency of the spectral peak), and the Phillips sea with shorter waves. In the Hasselmann sea, which contains up to 95 % of wave energy, a resonant nonlinear interaction dominates over generation of wave energy by wind. White-cap dissipation in the Hasselmann sea in negligibly small. The resonant interaction forms a flux of energy into the Phillips sea, which plays a role of a universal sink of energy. This theory is supported by massive numerical experiments and explains the majority of pertinent experimental facts accumulated in physical oceanography.

1. Introduction

We will start with the taken-for-granted aphorism that "there is nothing more practical than a good theory." Since the time of Galileo, physicists have tried to develop theoretical models of natural phenomena. They have succeeded for phenomena of very different scales: from the scale of elementary particles to the scale of the Universe. Geophysical phenomena - weather forecasting, prediction of earthquakes or origin of hurricanes - are intermediate in scale but not in complexity. As a rule, these phenomena are very difficult for theoretical investigation because there are too many factors involved. Creation of a theoretically justified analytic theory of wind-driven sea looks, at first glance, to be "mission impossible." Waves are generated by turbulent winds; these waves break, forming white caps, sprays, bubbles, etc. Nevertheless, the development of an adequate analytic theory of wind-driven sea is possible. The purpose of this paper is to demonstrate this possibility.

It is obvious that a wind-driven sea needs a statistical description. In the system under consideration, such a description can be performed efficiently if we have at least one small parameter. The absence of a small parameter makes

* Corresponding author. Tel.: +1-520-621-6892 ; fax: +1-520-621-8322.
  E-mail address: zakharov@math.arizona.edu

development of a good theory that describes turbulence in an incompressible fluid quite problematic. Fortunately, in the case of a wind-driven sea we can find two small parameters. The first one is the ratio of air and water densities, $\rho = \frac{\rho_a}{\rho_w} \sim 1.2 \times 10^{-3}$. Smallness of this parameter is responsible for the fact that generation of waves by wind is a slow process: development of an intense wave takes thousands of its periods. Another small parameter is the steepness, μ, defined as follows: $\mu^2(k_0) = \int_{|k|<k_0} k^2 \epsilon(k) dk$. Here $\epsilon(k)$ is the energy spectrum. Disastrously long and high waves of a strong storm are just gently sloping. A wave with steepness $\mu \simeq 0.1$ is considered by seafarers as dangerously steep. A typical value of steepness is $\mu \simeq 0.04 - 0.07$. Smallness of μ allows us to sort out the nonlinear interaction processes and determine the leading process, which is the four-wave resonant interaction. It was done by O. Phillips in 1960 [1]. A statistical description of weakly nonlinear waves can be accomplished by standard methods of theoretical physics. It was performed by K. Hasselmann in 1962-63 [2], [3]. He derived what we call the "Hasselmann kinetic equation," which became a new member of the big family of kinetic equations widely used in theoretical physics.

In spite of the fact that the mentioned seminal results were obtained long ago, the development of wind-wave theory was slow. Some important advances were achieved in research articles of late 1960's - 1980's [4-9] but they exerted little influence on development of the theory.

For half a century oceanographers have constructed operational models for wave forecasting. In these models, the tuning of parameters made it possible to improve the forecasting, but the use of heuristic models added little to the understanding of the physical processes that take place on the surface of wind-driven sea. During the last decade the analytical theory of wind-driven sea got a new life [10-19]. It became obvious that the majority of data obtained in physical experiments (in ocean and wave tanks) together with numerical experiments can be explained in a framework of a well-justified simple theory. The presented paper is a first brief systematic description of this theory. Its main points were reported at the Lorentz lecture on the AGU Fall meeting, December 2016, San Francisco.

The central point of the proposed analytical wind-driven sea theory is the following. Wind-driven waves can be separated into two ensembles: the Hasselmann sea and the Phillips sea. The Hasselmann sea contains long waves with frequencies $\omega < \omega_H$, $\omega_H \simeq 4 - 5 \omega_p$. Here ω_p is the frequency of the spectral peak. The Phillips sea consists of shorter waves. In the Hasselmann sea the waves are generated by wind, mostly near the spectral peak, but their spectral distribution is shaped by a resonant nonlinear interaction. This interaction throws the wave energy into the Phillips sea, where it dissipates due to breaking. We don't need to know the details of wave-breaking. The Phillips sea works as a universal sink that absorbs all energy sent there by resonant interactions. The white-cap dissipation inside the Hasselmann sea is negligibly small. This is a crucial point that makes possible to develop a self-sustained theory of the Hasselmann sea, which contains the bulk of the wave energy (up to 95 %).

2. Quasi-Conservative Hasselmann equation

It is accepted by the physical oceanography community (see, for example [20]) that deep water ocean gravity surface wave forecasting models are described by the Hasselmann equation [2, 3] This equation is also known as the kinetic equation for waves [4]. Sometimes it is called the Bolzmann equation [21] or energy balance equation [22].

$$\frac{\partial \epsilon}{\partial t} + \frac{\partial \omega_k}{\partial \mathbf{k}} \frac{\partial \epsilon}{\partial \mathbf{r}} = S_{nl} + S_{in} + S_{diss} \tag{1}$$

Here $\epsilon = \epsilon(\omega_k, \theta, r, t)$ is the wave energy spectrum. This spectrum is a function of wave frequency $\omega_k = \omega(k)$, angle θ, two-dimensional real space coordinate $r = (x, y)$, and time t. The terms S_{nl}, S_{in} and S_{diss} are the nonlinear, wind input and wave-breaking dissipation source terms. We will consider the deep water case only: the dispersion law is $\omega_k = \sqrt{gk}$, where g is the gravitational acceleration and $k = |\mathbf{k}|$ is the absolute value of the vector wavenumber $\mathbf{k} = (k_x, k_y)$. Since Hasselmann's work, Eq.(1) has become the basis of operational wave forecasting models.

While the physical oceanography community agrees on the general applicability of Eq. (1), there is no consensus on universal parameterizations of the source terms S_{nl}, S_{in} and S_{diss}. In this paper we put $S_{diss} = 0$. It is astonishing how many nontrivial facts extracted from field and numerical experiments confirm this statement [10],[12],[13]. Of course, $S_{diss} = 0$ only in the Hasselmann sea.

We start our consideration with the study of the quasi-conservative Hasselmann kinetic equation written for the wave action spectrum $N_{\mathbf{k}}(t)$.

$$\frac{dN}{dt} = S_{nl} \tag{2}$$

$$S_{\rm nl} = \pi g^2 \int\limits_{\mathbf{k}_1,\mathbf{k}_2,\mathbf{k}_3} (T_{\mathbf{k}\mathbf{k}_1\mathbf{k}_2\mathbf{k}_3})^2 \times (N_{\mathbf{k}}N_{\mathbf{k}_2}N_{\mathbf{k}_3} + N_{\mathbf{k}_1}N_{\mathbf{k}_2}N_{\mathbf{k}_3} - N_{\mathbf{k}}N_{\mathbf{k}_1}N_{\mathbf{k}_2} - N_{\mathbf{k}}N_{\mathbf{k}_1}N_{\mathbf{k}_3}) \times$$

$$\times \delta(\mathbf{k} + \mathbf{k}_1 - \mathbf{k}_2 - \mathbf{k}_3)\,\delta(\omega + \omega_1 - \omega_2 - \omega_3) \times d\mathbf{k}_1\,d\mathbf{k}_2\,d\mathbf{k}_3 \tag{3}$$

The energy spectrum $\epsilon(k)$ is connected with wave action spectrum by relation $\epsilon(k) = \frac{1}{2}\omega_k(N_k + N_{-k})$. Here $\omega(k) = \sqrt{gk}$ is the dispersion law. The coefficient $T_{kk_1k_2k_3}$ in Eq. (3) is the coupling coefficient introduced in [23], [24]:

$$T_{\mathbf{k}_1\mathbf{k}_2\mathbf{k}_3\mathbf{k}_4} = \frac{1}{2}\left(\hat{T}_{\mathbf{k}_1\mathbf{k}_2\mathbf{k}_3\mathbf{k}_4} + \hat{T}_{\mathbf{k}_3\mathbf{k}_3\mathbf{k}_1\mathbf{k}_2}\right)$$

$$\hat{T}_{\mathbf{k}_1\mathbf{k}_2\mathbf{k}_3\mathbf{k}_4} = -\frac{1}{4}\frac{1}{(k_1k_2k_3k_4)^{1/4}}\left\{ \frac{1}{2}\left(k_{1+2}^2 - (\omega_1 + \omega_2)^4\right) \times \left(\mathbf{k}_1\mathbf{k}_2 - k_1k_2 + \mathbf{k}_3\mathbf{k}_4 - k_3k_4\right)\right.$$

$$-\frac{1}{2}\left(k_{1-3}^2 - (\omega_1 - \omega_3)^4\right) \times \left(\mathbf{k}_1\mathbf{k}_3 + k_1k_3 + \mathbf{k}_2\mathbf{k}_4 + k_2k_4\right)$$

$$-\frac{1}{2}\left(k_{1-4}^2 - (\omega_1 - \omega_4)^4\right) \times \left(\mathbf{k}_1\mathbf{k}_4 + k_1k_4 + \mathbf{k}_2\mathbf{k}_3 + k_2k_3\right)$$

$$+\left(\frac{4(\omega_1 + \omega_2)^2}{k_{1+2} - (\omega_1 + \omega_2)^2} - 1\right) \times (\mathbf{k}_1\mathbf{k}_2 - k_1k_2)(\mathbf{k}_3\mathbf{k}_4 - k_3k_4)$$

$$+\left(\frac{4(\omega_1 - \omega_3)^2}{k_{1-3} - (\omega_1 - \omega_3)^2} - 1\right) \times (\mathbf{k}_1\mathbf{k}_3 + k_1k_3)(\mathbf{k}_2\mathbf{k}_4 + k_2k_4)$$

$$\left. +\left(\frac{4(\omega_1 - \omega_4)^2}{k_{1-4} - (\omega_1 - \omega_4)^2} - 1\right) \times (\mathbf{k}_1\mathbf{k}_4 + k_1k_4)(\mathbf{k}_2\mathbf{k}_3 + k_2k_3)\right\} \tag{4}$$

Here k_{1+2}, k_{1-3} and k_{1-4} are the moduli of the $\mathbf{k}_1 + \mathbf{k}_2$, $\mathbf{k}_1 - \mathbf{k}_3$ and $\mathbf{k}_1 - \mathbf{k}_4$ vectors respectively. It should be stressed that we need to know the coupling coefficient at the resonant manifold only:

$$\mathbf{k}_1 + \mathbf{k}_2 = \mathbf{k}_3 + \mathbf{k}_4; \qquad \omega_1 + \omega_2 = \omega_3 + \omega_4 \tag{5}$$

The coupling coefficient satisfies the symmetry conditions $T_{1234} = T_{2134} = T_{1243} = T_{3412}$. Now suppose that the wave vectors $\mathbf{k}_1$ and $\mathbf{k}_3$ are much shorter than the wave vectors $\mathbf{k}_2$ and $\mathbf{k}_4$. Taking Eq. (5) into account we see that $\mathbf{k}_1$ and $\mathbf{k}_3$ have nearly equal length. Vectors $\mathbf{k}_2$ and $\mathbf{k}_4$ are nearly equal, both in length and direction. An example of such configuration is shown on Fig. 1.
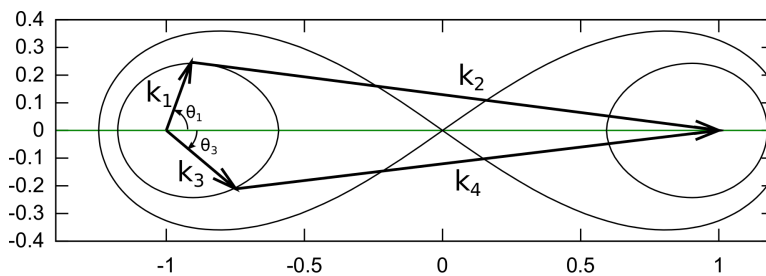

Fig. 1. A wave vector quadruplet of a long-short interaction. A curve $\omega_1 + \omega_2 = $ const is drawn; any two points of the curve constitute a resonant quadruplet. The θ_1 and θ_3 angles are given with respect to the vector $\mathbf{k}_1 + \mathbf{k}_2 = \mathbf{k}_3 + \mathbf{k}_4$. The eight-shape figure is the Phillips curve.

Let us underline one important property of the resonant manifold (5). Suppose that the three wave vectors, k_1, k_2, k_3 in (5) are bound in length by some number $|k_i| < k_0$, $i = 1, 2, 3$. However, the last term in (5) might have a longer absolute value. In fact, in virtue of (5) we have $|k_1| < 5/4\,k_0$.

Hereafter we define $k_1 = |\mathbf{k}_1|$, $k_2 = |\mathbf{k}_2|$, etc. We have $k_1 \approx k_3 \ll k_2 \approx k_4$. After tedious algebra one may find the following asymptotic behavior for the coupling coefficient:

$$T_{\mathbf{k}_1,\mathbf{k}_2,\mathbf{k}_3,\mathbf{k}_4)} \rightarrow \frac{1}{2}k_1^2 k_2 T_{\theta_1\theta_3}, \qquad T_{\theta_1\theta_3} = (\cos\theta_1 + \cos\theta_3)(1 + \cos(\theta_1 - \theta_3))$$

Here θ_1 is the angle between the small vector $\mathbf{k}_1$ and $\mathbf{k}_1 + \mathbf{k}_2$ (see Fig. 1); the same stands for θ_3.

In the diagonal case $\theta_1 = \theta_3$, $\mathbf{k}_1 = \mathbf{k}_3$, $\mathbf{k}_2 = \mathbf{k}_4$.

$$T(\mathbf{k}_1, \mathbf{k}_2) = 2k_1^2 k_2 \cos(\theta_1) \tag{6}$$

A systematic derivation of the nonlinear term S_{nl} is described in detail in [25]. The expression for the coupling coefficient presented in that paper differs from Eq. (4), however on the resonant manifold Eq. (5) both expressions coincide.

The derivation of the Hasselmann equation is based on the assumption that the total steepness μ is small. In fact, one must demand that $\mu(k_0) < 0.1$. In the real sea, the steepness $\mu(k_0)$ is a function growing with k_0. This means that Hasselmann equation is only valid inside the limited spectral band $0 < \omega < (4 - 6)\omega_p$, where ω_p is the frequency of the spectral peak. It is fortunate that in a typical case this "allowed" band contains more than 95% of the wave energy.

We should stress one important point. The Hasselmann equation is derived not for the real observable energy spectrum but for the "refined" spectrum cleared of "slave harmonics." This question is studied in detail in [14], [15]. It is shown there that "slave harmonics" can be neglected only in the case of very small steepness, $\mu \ll 1$. This is correct for long enough waves, but in the small-scale spectral area ($k > 20 \sim 30k_p$) the contribution of slave harmonics becomes dramatically more important. This fact is supported by direct phase-resolving numerical experiments [26], [27], [28], [29]. In this spectral area, the sea is a mixture of "leading harmonics" obeying the dispersion law $\omega \simeq \sqrt{gk}$ and slave harmonics that have combined frequencies. Also, in this spectral area we can observe either the formation of parasitic capillary ripples (for small wind velocity, $v < 3 \sim 5 m/sec$) or intensive wave breaking (for stronger wind).

For strong enough wind we can separate wind-driven sea into two parts: the "Hasselmann sea" with long waves and the "Phillips sea" with shorter waves. This question was studied theoretically in [30] and numerically in [27]. Can we "improve" the Hasselmann equation to make it applicable to description of the Phillips sea? The answer to this question is still open.

Another important point is the question of conservation laws. The widely accepted opinion is that the quasi-conservative Hasselmann equation Eq. (2) has basic conservation laws, i.e. wave action, energy and momentum:

$$N = \int N_k \, dk, \qquad E = \int \omega_k N_k \, dk, \qquad \mathbf{M} = \int \mathbf{k} N_k \, dk$$

Another widely accepted opinion is the following: A wave field cannot gain or loose energy through resonant interaction; growth or loss of wave action, momentum or energy must therefore take place through other processes such as wind input, whitecapping or bottom interaction (see, for example Chapter II in the well-known book "Dynamics and Modelling of Ocean Waves" [31]. This statement is gravely erroneous. Certainly, the resonant interaction cannot gain energy, but this interaction provides for the loss of energy and momentum into the spectral area of infinitely small scales. This process really occurs and takes a leading role in establishing the energy and momentum balance in the wind-driven sea.

Let us study more carefully the conservation laws. Apparently

$$\frac{dE}{dt} = \int \omega_k S_{nl} \, dk \tag{7}$$

If we boldly perform the permutation of integration order in Eq. (7) we will end up with relation

$$\begin{aligned}
\frac{dE}{dt} &= \pi g^2 \int |T_{kk_1 k_2 k_3}|^2 N_{k_1} N_{k_2} N_{k_3} \times (\omega_k + \omega_{k_1} - \omega_{k_2} - \omega_{k_3}) \delta(\omega_k + \omega_{k_1} - \omega_{k_2} - \omega_{k_3}) \times \\
&\times \delta(\mathbf{k} + \mathbf{k}_1 - \mathbf{k}_2 - \mathbf{k}_3) \, d\mathbf{k} \, d\mathbf{k}_1 \, d\mathbf{k}_2 \, d\mathbf{k}_3
\end{aligned} \tag{8}$$

It seems that Eq. (7) means that $dE/dt = 0$, but this would be correct only if all terms in this relation are finite and represented by convergent integrals. Now assume that N_k has asymptotic behavior $N_k \to 1/k^4$, $k \to \infty$. Then all terms in Eq. (7) will diverge logarithmically and will actually be infinite. Different terms in $d\mathbf{M}/dt$ will diverge even worse. Thus, in the presence of spectral tails, the conservation of energy and momentum fails. The asymptotic behavior $N_k \sim 1/k^4$ means that $I_k \simeq k^{-5/2}$ and $F(\omega) \simeq \omega^{-4}$. These spectra are commonly observed in the wind-driven sea in the spectral range $\omega_p < \omega < 5\omega_p$, where ω_p the is frequency of the spectral peak.

Let us add a little piece of pure mathematics. Strictly speaking, even the simple Eq. (7) is not correct. Permutation of integration order in multi-dimensional integrals is allowed under strict limitations that are dictated by the so-called "Fubini theorem." In our case this theorem demands that action spectra should decay fast enough at $k \to \infty$:

$$N(k) < \frac{c}{k^{25/6+\epsilon}}, \quad \epsilon > 0$$

This means that the energy spectrum $F(\omega)$ must decay faster than $\omega^{-13/3}$. In the short-scale region of a real sea we usually observe the Phillips spectrum $F(\omega) \simeq \alpha g^2/\omega^5$. Because $5 > 13/3$ the integrals are conserved.

Let us notice that this takes place in the Phillips sea, consisting of short waves ($\omega > \omega_H$), outside of the Hasselmann sea, consisting of long waves ($\omega < \omega_H \sim 5\omega_p$). The resonant nonlinear interaction throws energy and momentum from the Hasselmann sea into the Phillips sea. Thus:

$$P = -\int_0^{2\pi} d\theta \int_0^{\omega_H} \frac{d\epsilon(\omega, \theta)}{dt} d\omega, \quad R_x = -\frac{1}{g} \int_0^{2\pi} d\theta \int_0^{\omega_H} \omega \cos\theta \frac{d\epsilon(\omega, \theta)}{dt} d\omega$$

P and R_x are fluxes of energy and momentum from the Hasselmann sea into the Phillips sea. Because they are not zero, one can call Eq. (2) a quasi-conservative equation. Notice, that Eq. (2) is a natural model for study of the ocean swell evolution. We have solved this equation numerically and have observed a permanent loss of energy and momentum [44].

3. Kolmogorov-type spectra

Let us study isotropic solutions of the stationary quasi-conservative Hasselmann equation:

$$S_{nl} = 0 \tag{9}$$

We assume that the solution of Eq. (8) is a powerlike function $N = ak^{-x}$. Then

$$S_{nl} = a^3 g^{\frac{3}{2}} k^{-3x+\frac{19}{2}} F(x)$$

where F is a dimensionless function depending on x only.

It was shown in [6], [32] that $F(x) = 0$ at the two points $x = 4$ and $x \simeq 23/6$ only. This is a strict mathematical theorem, which is supported by careful numerical experiments [33], [12], [13]. Integrals in Eq. (9) converge if $5/2 < x < 19/4$ [19]. Function F is shown on Fig. 2.
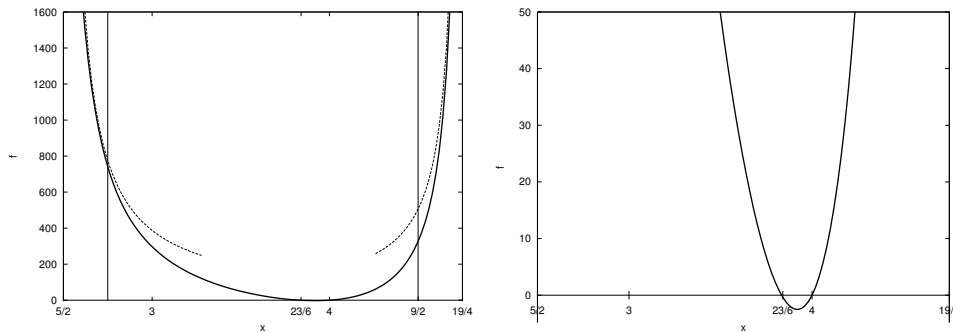

Fig. 2. F function graph and its asymptotes. The second picture is the closeup of the function zeroes.

This means that Eq. (9) has exactly two powerlike solutions:

$$N_k^{(1)} = c_p \frac{P_0^{1/3}}{g^{2/3}} \frac{1}{k^4}, \qquad N_k^{(2)} = c_q \frac{Q_0^{1/3}}{g^{1/2}} \frac{1}{k^{23/6}}. \tag{10}$$

Here P_0 is the energy flux and Q_0 is the wave action flux. The dimensionless constants c_p and c_q are defined from the first derivatives of F

$$c_p = \left(\frac{3}{2\pi F'(4)}\right)^{1/3}, \qquad c_q = \left(-\frac{3}{2\pi F'(23/6)}\right)^{1/3}$$

Our numerical calculation of the derivatives of F at $x = 4$ and $x = 23/6$ gives

$$c_p = 0.203, \quad c_q = 0.194 \tag{11}$$

One can mention that the "unidirectional" (integrated by angle) energy spectra $E(\omega)$ are connected with the isotropic wave action spectra by the relation

$$F(\omega)\,d\omega = 2\pi\omega_k N_k k\,dk \tag{12}$$

Hence we find the following exact solutions of Eq. (9):

$$F_1(\omega) = \frac{4\pi c_p}{\omega^4} g^{4/3} P_0^{1/3} \tag{13}$$

This expression is known as the Zakharov-Filonenko spectrum and was found in 1966 [4]. It is a Kolmogorov-type spectrum that presumes the presence of a source of energy $P_0 = d\epsilon/dt$ at $k = 0$. This is the spectrum of "direct inverse cascade" similar to the classical Kolmogorov spectrum in the theory of turbulence in a three-dimensional incompressible fluid. The second spectrum first introduced in [5], [6] is the following:

$$F_2(\omega) = \frac{4\pi c_q}{\omega^{11/3}} g\, Q_0^{1/3} \tag{14}$$

It describes the "inverse cascade" of wave action, and can be compared with the Kolmogorov spectrum of the energy inverse cascade in the theory of turbulence in a two-dimensional incompressible fluid.

The existence of solutions of Eq. (8) originates from possibility of splitting S_{nl} as follows:

$$S_{nl} = F_k - \Gamma_k N_k, \tag{15}$$

where

$$F_k = \pi g^2 \int |T_{kk_1k_2k_3}|^2\, \delta(k + k_1 - k_2 - k_3)\, \delta(\omega_k + \omega_{k_1} - \omega_{k_2} - \omega_{k_3})\, N_{k_1} N_{k_2} N_{k_3}\, dk_1 dk_2 dk_3 \tag{16}$$

and Γ_k, the dissipation rate due to the presence of four-wave processes, is the following:

$$\Gamma_k = \pi g^2 \int |T_{kk_1,k_2k_3}|^2\, \delta(k + k_1 - k_2 - k_3)\, \delta(\omega_k + \omega_{k_1} - \omega_{k_2} - \omega_{k_3}) \times$$
$$\times (N_{k_1} N_{k_2} + N_{k_1} N_{k_3} - N_{k_2} N_{k_3})\, dk_1 dk_2 dk_3. \tag{17}$$

One can call F_k the "income term" and $\Gamma_k N_k$ the "outcome term". Solutions of Eq. (8) are the result of competition between the income and outcome terms. In statistical physics the separate study of income and outcome terms is a routine procedure. In stationarity they compensate each other, and this is the "principle of detailed equilibrium". Competition of these terms leads to the establishment of of stationary thermodynamic equilibrium spectra like the Maxwell distribution in the kinetic theory of gases or the Plank distribution in optics and physics of condensed matter. It is important to mention that Eq. (2) is the limiting case of a more general quantum kinetic equation for bosonic quasiparticles derived by Nordheim in 1929 [34]. Kolmogorov-type spectra of the Nordheim equation were studied by Y.V. Lvov et al [35].

There is one more reason why the splitting of S_{nl} is so useful. First of all, it explains why the conservation laws in reality do not conserve. Suppose, in the initial moment of time, $N(k) = 0$. Thus $S_{nl} > 0$ in the spectral area $k_0 < |k| < 5/4\,k_0$. As a result, energy inside the area $|k| < k_0$ decreases in time. This fact is very important in connection with numerical solution of equation (2). Any numerical scheme provides that frequency varies in a bounded interval

$0 < \omega < \omega_{max}$ and automatically provides the leakage of energy outside the area $\omega < \omega_{max}$. A good numerical experiment can be performed in the absence of all S_{diss}.

We can expect that Eq. (8) has thermodynamic equilibrium solutions, the Rayley-Jeans spectra

$$\epsilon(k) = \frac{T}{\omega_k + \mu}$$

Here T is temperature and μ is chemical potential. However these solutions have no physical meaning because a real sea is very far from thermodynamic equilibrium. Moreover, the substitution of thermodynamic spectra into S_{nl} leads to bad divergences of integrals. It is important to stress that the spectra (13) and (14) are the simplest examples of exact solution of Eq. (9). To outline a broader class of its solutions one can introduce the elliptic differential operator [14]:

$$L f(\omega, \phi) = \left(\frac{\partial^2}{\partial \omega^2} + \frac{2}{\omega^2} \frac{\partial^2}{\partial \phi^2} \right) f(\omega, \phi) \tag{18}$$

with following parameters: $0 < \omega < \infty, \ 0 < \phi < 2\pi$. The equation

$$L G = \delta(\omega - \omega') \delta(\phi - \phi') \tag{19}$$

with boundary conditions $G|_{\omega \to 0} = 0$, $G_{\omega \to \infty} < \infty$, $G(2\pi) = G(0)$ can be resolved as

$$G(\omega, \omega', \phi - \phi') = \frac{1}{4\pi} \sqrt{\omega \omega'} \sum_{n=-\infty}^{\infty} e^{in(\phi - \phi')} \times \left[\left(\frac{\omega}{\omega'} \right)^{\Delta_n} \Theta(\omega' - \omega) + \left(\frac{\omega'}{\omega} \right)^{\Delta_n} \Theta(\omega - \omega') \right], \tag{20}$$

where $\Delta_n = 1/2 \sqrt{1 + 8n^2}$. Now we define:

$$A(\omega, \phi) = \int_0^\infty d\omega' \int_0^{2\pi} d\phi' \, G(\omega, \omega', \phi - \phi') \, S_{nl}(\omega', \phi'). \tag{21}$$

Then Eq. (2) takes the following form

$$\frac{\partial N}{\partial t} = L A \tag{22}$$

and the stationary equation is

$$L A = 0 \tag{23}$$

The operator A is a regular integral operator. This fact leads to a bold idea. If we assume that

$$A = \frac{H_0}{g^4} \omega^{15} N^3, \tag{24}$$

then the nonlinear term S_{nl} turns into the elliptic operator:

$$S_{nl} = \frac{H_0}{g^4} \left(\frac{\partial^2}{\partial \omega^2} + \frac{2}{\omega^2} \frac{\partial^2}{\partial \phi^2} \right) \omega^{15} N^3. \tag{25}$$

This is a so-called "diffusion approximation", first introduced in article [23] and later on developed in [36]. In spite of being very simple, this approximation grasps the basic features of the wind-driven sea theory. We will refer mostly to this model, having in mind that the real case Eq. (21) does not differ much from it, at least qualitatively.

H_0 is a dimensionless tuning constant. In Eq. (22), $N = N(\omega, \phi)$, $\epsilon(\omega, \phi) = \omega N(\omega, \phi)$. Eq. (25) has the following anisotropic KZ solution

$$A = \frac{1}{2\pi g} \left\{ P + \omega Q + \frac{R_x}{\omega} \cos \phi \right\}, \tag{26}$$

where P and R_x are fluxes of energy and momentum as $\omega \to \infty$ and Q is the flux of wave action directed to small wave numbers. In a general case, Eq. (21) is a nonlinear integral equation; however in the diffusion approximation the KZ solution can be found in the explicit form:

$$N(\omega, \phi) = \frac{1}{(2\pi H_0)^{1/3}} \frac{g}{\omega^5} \left(P + \omega Q + \frac{R_x}{\omega} \cos\phi \right)^{1/3}. \tag{27}$$

By comparison with (11) we easily find that in this case

$$c_p = c_q = \frac{1}{2(2\pi H_0)^{1/3}} = 0.199, \qquad H_0 = 2.57.$$

This is exactly the arithmetic mean between the values of Kolmogorov constants given by (11).

By multiplication of Eq. (27) by $2\pi\omega$ we get the general KZ spectrum in the diffusion approximation:

$$F(\omega) = 2.78 \frac{g^{4/3}}{\omega^4} \left(P + \omega Q + \frac{R_x}{\omega} \cos\phi \right)^{1/3}. \tag{28}$$

For the real sea, Eq. (23) is a nonlinear integral equation which can be solved numerically only. The "toy" diffusion model allows us to find the explicit equation for the KZ-solution which grasps the main features of real solution. One can assert that the real KZ solution is

$$F(\omega) = \frac{g^{4/3} P^{1/3}}{\omega^4} R \left(\frac{\omega Q}{P}, \frac{R_x}{g\,\omega\,P}, \phi \right) \tag{29}$$

In the limit $P \to 0$, $R_x \to 0$ we have $R \to 4\pi c_p$. In the limit $R_x = 0$, $P \to 0$

$$R \to 4\pi c_q \left(\frac{\omega Q}{P} \right)^{1/3}$$

We have to mention that Q is the flux of wave action coming from the spectral area of very small scales. In the majority of physical situations one can put $Q = 0$. From the physical viewpoint the most interesting case is $Q = 0$, for which

$$F(\omega) = \frac{g^{4/3} P^{1/3}}{\omega^4} R_0 \left(\frac{R_x}{g\,\omega\,P}, \phi \right) \tag{30}$$

Here R_0 is an unknown function that we believe describes the angular spreading of wave spectra. It was shown long ago [37] that as $\omega \to 0$

$$R_0 \to 4\pi c_p \left(1 + \frac{\lambda R_x}{g\,\omega\,P} \cos\phi + \cdots \right) \tag{31}$$

where λ is a dimensionless constant. In the "toy" diffusion model $\lambda = 1/3$. We should stress that all KZ spectra are isotropic in the limit $\omega \to \infty$ and are very close to $F(\omega) \sim 1/\omega^4$.

Let us return to the representation of S_{nl} in the "split" form (15). Apparently the solution of the equation $S_{nl} = 0$ is given by the expression

$$N_k = \frac{F_k}{\Gamma_k} \tag{32}$$

For KZ-spectra both F_k, Γ_k diverge as $k \to \infty$. However these divergences are cancelled.

A detailed numerical study of the function $R_0(\frac{R_x}{g\,\omega,P}, \phi)$ and its comparison with observed in experiments angular spectra is the problem of most importance in our agenda.

4. Energy balance in wind-driven sea

To answer the most painful question - which source terms in Eq. (1) are dominant? - one should present S_{nl} in the split form. This is clear to any physicist (pity, not to oceanographers). After the splitting, Eq. (1) takes the following form:

$$\frac{\partial N}{\partial t} + \frac{\partial \omega_k}{\partial k}\frac{\partial N}{\partial r} = F_k - \Gamma_k N_k + S_{in} + S_{diss}$$

In fact, the forcing terms S_{in} and S_{dis} are not known well enough; thus it is reasonable to accept the simplest models of both terms assuming that they are proportional to the action spectrum:

$$S_{in} = \gamma_{in}(k)\,N(k), \quad S_{dis} = -\gamma_{dis}(k)\,N(k). \tag{33}$$

Hence

$$\gamma(k) = \gamma_{in}(k) - \gamma_{dis}(k). \tag{34}$$

In reality $\gamma_{dis}(k)$ depends dramatically on the overall steepness μ. So far, let us notice that the stationary balance equation can be written in the form

$$F_k - \Gamma_k N_k + \gamma_k N = 0 \tag{35}$$

Definitions of Γ_k and F_k are given by Eq. (16) and Eq. (17).

The stationary solution of Eq. (1) is the following:

$$N_k = \frac{F_k}{\Gamma_k - \gamma_k}. \tag{36}$$

The positive solution exists if $\Gamma_k > \gamma_k$. The term Γ_k can be treated as the nonlinear damping that appears due to four-wave interaction. In the presence of nonlinear damping the dispersion relation must be renormalized

$$\omega_k \to \omega_k + \frac{1}{2}\int T_{kk_1kk_1} N_k\,dk + i\Gamma_k$$

The main point of the proposed theory is that the nonlinear dumping has a very powerful effect. In reality, $\Gamma_k \gg \gamma_k$. A "naive" dimensional consideration gives

$$\Gamma_k \simeq \frac{4\pi g^2}{\omega_k}\,k^{10}\,N_k^2, \tag{37}$$

However, this estimate works only if $k \simeq k_p$, where k_p is the wave number of the spectral maximum.

Let $k \gg k_p$. Then for Γ_k we get

$$\Gamma_k = 2\pi g^2 \int |T_{kk_1,kk_3}|^2\,\delta(\omega_{k_1} - \omega_{k_3})\,N_{k_1}N_{k_3}\,dk_1 dk_2. \tag{38}$$

The main source of Γ_k is the interaction of long and short waves. To estimate Γ_k more accurately, we assume that the spectrum of long waves is narrow in angle, $N(k_1, \theta_1) = \tilde{N}(k_1)\,\delta(\theta_1)$. Long waves propagate along the axis x, and $\vec{k}$ is the wave vector of short wave propagating in direction θ. For the coupling coefficient we can use the asymptotic Eq. (6) and obtain

$$\Gamma_k = 8\pi g^{3/2}\,k^2\,\cos^2\theta \int_0^\infty k_1^{13/2}\,\tilde{N}^2(k_1)\,dk_1. \tag{39}$$

Even for the most mildly decaying KZ spectrum, $N_k \simeq k^{-23/6}$, the integrand behaves like $k_1^{-7/6}$ and the integral converges as $k \to \infty$. Thus the main contribution in (39) is given by $k_1 \sim k_p$. For an accurate estimate of Γ_k we need to know the detailed structure of the spectrum near the spectral peak. Let us make the most "mild assumption" and
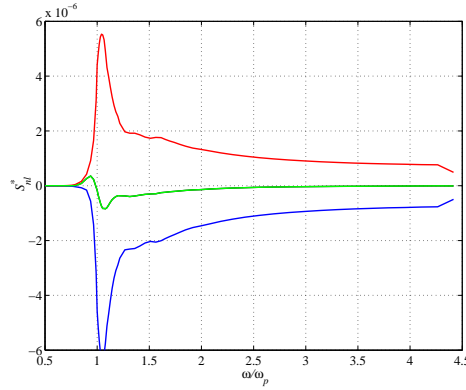
Fig. 3. Split of nonlinear interaction term S_{nl} (central curve) into F_k (upper curve) and $\Gamma_k N_k$ (lower curve)

consider that there is no peakedness and the spectrum looks like the Pierson-Moscowitz spectrum of a "mature sea" [38]:

$$N_k \simeq \frac{3}{2} \frac{E}{\sqrt{g}} \frac{k_p^{3/2}}{k^4} \theta(k - k_p). \tag{40}$$

Here E is the total energy. By plugging Eq. (40) into Eq. (39) we get the equation

$$\Gamma_\omega = 36 \pi \omega \left(\frac{\omega}{\omega_p} \right)^3 \mu_p^4 \cos^2 \theta, \quad \mu_p^2 = \frac{g^2 E}{\omega p^4} \tag{41}$$

that includes a huge enhancing factor: $36\pi \simeq 113.04$. For very modest value of steepness, $\mu_p \simeq 0.05$, we get

$$\Gamma_\omega \simeq 7.06 \cdot 10^{-4} \omega \left(\frac{\omega}{\omega_p} \right)^3 \cos^2 \theta. \tag{42}$$

In the real sea the spectra usually have "peakedness" which enhances (39) essentially. We must underline that the splitting of S_{nl} can be studied numerically. We have modified the well-known Resio-Tracy code for solving the Hasselmann equation to calculate competing terms F_k and $\Gamma_k N$ separately [15]. A typical splitting is shown in Fig. 3. For a nonlinear interaction term $S_{nl} = F_k - \Gamma_k N_k$, the magnitudes of the constituents F_k and $\Gamma_k N_k$ essentially exceed their difference. They are one order higher than the magnitude of S_{nl}.

The dominance of S_{nl} was not apparent for two reasons. First, it is not correct to compare S_{nl} and S_{in}; instead one should compare Γ_k and γ_k. Second, the widely accepted models for S_{diss} overestimate dissipation due to white capping. As a result, the dominance of S_{nl} is masked.

Concerning interaction with wind, at the moment there are at least a dozen models for $\Gamma(k) = \gamma(\omega, \phi)$. Some of them are derived by the use of conflicting theoretical models; others are taken from experimental data. None of the proposed models are convincing. They are essentially different and the scatter is very large, $300 - 500\,\%$. A critical review of different models is presented in [27].

The dimensionless quantities $\gamma/\omega \times 10^3$ as functions of dimensionless frequency $\omega u_{10}/g$ are plotted on Fig. 4 taken from [12].

We pay special attention to two models:

1. The Plant model [39] $\gamma = 0.03 \frac{\rho_a}{\rho_\omega} \omega \left(\frac{\omega U}{g} \right)^2 \cos \phi, \qquad \cos \phi > 0$

2. ZRP model [17] $\quad \gamma = 0.05 \frac{\rho_a}{\rho_\omega} \omega \left(\frac{\omega U}{g} \right)^{4/3} \cos^2 \phi, \qquad -\pi/2 < \phi < \pi/2$

In both models $\gamma \simeq \omega^{1+s}$ is a powerlike function on frequency.

Comparison of all known models for S_{in} with the nonlinear dumping term Γ_k calculated according to Eq. (17) is presented on Fig. 5 One can see that Γ_k, at least in order of magnitude, is larger than $\gamma_{in}(k)$. This figure conspicuously demonstrates that the nonlinear wave interaction is the leading term in the energy balance of a wind-driven sea.
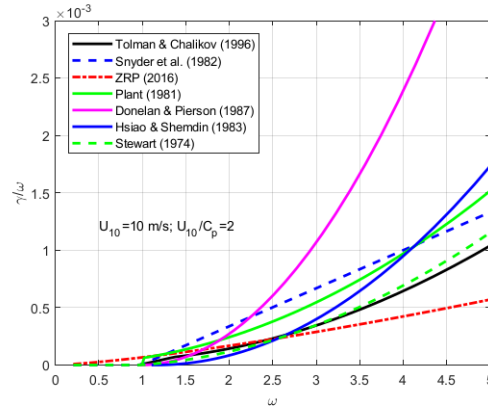
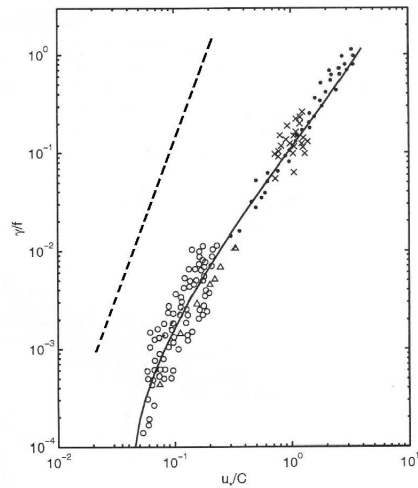Fig. 4. Dimensionless wind input for $u_{10} = 10 m/sec$.

Fig. 5. Comparison of experimental data for the wind-induced growth rate $2\pi \gamma_{in}(\omega)/\omega$ taken from [14], [15] and the damping due to four-wave interactions $2\pi \Gamma(\omega)/\omega$, calculated for narrow in angle spectrum at $\mu \simeq 0.05$ using Eq. (42) (dashed line)

5. Experimental evidence of S_{nl} domination

In the previous chapter we have shown analytically and numerically that the S_{nl} term dominates over the S_{in} term. Because in the Hassenlmann sea the term S_{diss} cannot be stronger than γ_{in} (otherwise waves would not be excited), the term S_{nl} dominates over both. Both the source term and the nonlinear wave interaction are the dominating physical processes that take place in a wind-driven sea.

This fact is supported by convincing experimental data collected in a broad ranges of wind velocities: $3m/sec < U, 30m/sec$. Following Kitaigorodski [40], hereafter we will use the dimensionless duration and fetch, as well as the dimensionless frequency and energy:

$$\tau = \frac{tg}{U}, \quad \chi = \frac{xg}{U^2}, \quad \sigma = \frac{\omega U}{g}, \quad F = \frac{\epsilon g^2}{U^4} \tag{43}$$

Also, we introduce integral dimensionless quantities

$$\tilde{F} = \int_0^\infty F(\sigma)d\sigma, \qquad \tilde{\sigma} = \frac{1}{\tilde{F}} \int_0^\infty \sigma F(\sigma)d\sigma \tag{44}$$

The steepness of the main energy capacity wave can be estimated as follows

$$\mu_p \simeq \tilde{F}\,\tilde{\sigma}^4 \tag{45}$$

During the last seven decades many experiments measuring energy spectra of a wind-driven sea and its integral characteristics were performed in laboratory, on lakes, and in the different parts of the ocean. The most significant experiments were conducted in the "fetch dominating frame," where the sea is stationary in time and the wind has the opposite direction. In these challenging and expensive experiments, $\tilde{F}$ and $\tilde{\sigma}$ were measured as functions of fetch only: $\tilde{F} = \tilde{F}(\chi)$, $\tilde{\sigma} = \tilde{\sigma}(\chi)$. All experimenters unanimously agree that $\tilde{F}$ and $\tilde{\sigma}$ are powerlike functions

$$\tilde{F} = \epsilon_0 \chi^p, \qquad \tilde{\sigma} = \omega_0 \chi^{-q} \tag{46}$$

Exponents p, q are different in different experiments. They vary inside the following ranges

$$0.7 < p < 1.1 \qquad 0.22 < q < 0.33 \tag{47}$$

Suppose that F obeys the stationary Hasselmann equation. After transition to dimensionless variable this equation reads

$$\frac{\cos\theta}{2\sigma}\frac{\partial F}{\partial \chi} = S_{nl} + \gamma_{in}(\sigma)\,F \tag{48}$$

We include in Eq. (48) the interaction with wind. Let us make a very crude estimate of the different terms in this equation. Neglecting the wind input term we come to the following balance relation

$$\frac{F}{\tilde{\sigma}\chi} \simeq \tilde{\sigma}\,F\,\mu_p^4$$

or, after cancelling F and using Eq. (45)

$$\chi\tilde{F}^2\,\tilde{\sigma}^{10} \simeq 1 \tag{49}$$

Substituting (46) into Eq. (49) one can see that dependance on χ drops out if the exponents p, q are connected by the relation

$$10q - 2p = 1 \tag{50}$$

We call it the "magic relation." In virtue of this relation

$$q = q_{th} = \frac{2p+1}{10}$$

Moreover, from condition (49) we can conclude that $s = \epsilon_0^{1/5}\,\omega_0$ is a universal constant. Comparison with numerical experiments show that

$$s = \epsilon_0^{1/5}\,\omega_0 \simeq 1 \tag{51}$$

Results of 23 experiments performed in the open sea and Lake Michigan are presented in Table 1, which represents the majority (but not all) of the field experiments collected in physical oceanography for almost half of a century. References can be found in [13]. Experimental data are compared with predictions of the analytic theory presented in the present paper. According to theory, the exponents q_{chi} must coincide with the theoretically predicted value $q_{th} = 2p_\chi + 1/10$. One can see that the relative difference $\delta q \simeq \frac{1}{q_\chi}|q_\chi - q_{th}|$ does not exceed 10%. According to theory, the dimensionless quantity $s = \epsilon_0^{1/5}\,\omega_0$ must be a universal constant of order one. More accurate theoretical value of s (which is actually a slow varying function of p) will be presented shortly. Table 1 shows that experimentally measured values of s are close to unit. The data accumulated in Table 1 support theory very well.

One can add to Table 1 the composite data presented by I.R. Young in monograph [21] on page 105. This is a result obtained by the author by averaging over many field experiments. According to Young:

$$p_x = 0.8 \quad q_x = 0.25 \quad \epsilon_0 = 7.5 \cdot 10^{-7} \quad \omega_0 = 12.56 \quad s = 0.75$$

Table 1. Comparison of experimental data and predictions of theory

	Case	$\varepsilon_0 \times 10^7$	p_χ	ω_0	q_χ	q_{th}	S
1	Wen. et al. (1989)	18.900	0.700	10.40	0.23	0.24	0.75
2	Romero & Melville (2009) stabl	9.230	0.740	8.93	0.22	0.25	0.55
3	Donelan et al. (1985) var. der	8.410	0.760	11.60	0.23	0.25	0.71
4	Dobson et al. (1989) wind. int	12.700	0.750	10.68	0.24	0.25	0.71
5	Kahma & Calkoen (1992) stabl	9.300	0.760	12.00	0.24	0.25	0.75
6	Evans & Kibblewhite (1990) stra	5.900	0.786	16.27	0.28	0.26	0.92
7	Romero & Melville (2009) unstab	5.750	0.810	10.64	0.23	0.26	0.60
8	Hwang & Wang (2004)	6.191	0.811	11.86	0.24	0.26	0.68
9	SMB CERC (1977) by Young	7.820	0.840	10.82	0.25	0.27	0.65
10	Davidan (1996), U_{10} scaling	5.550	0.840	16.34	0.29	0.27	0.92
11	Evans & Kibblewhite (1990) neut	2.600	0.872	18.72	0.30	0.27	0.90
12	Black. Sea	4.410	0.890	15.14	0.28	0.28	0.81
13	Kahma & Calkoen (1992) composit	5.200	0.900	13.70	0.27	0.28	0.76
14	Kahma & Pettersson (1994)	5.300	0.930	12.66	0.28	0.29	0.70
15	Kahma & Calkoen (1992) unstab	5.400	0.940	14.20	0.28	0.29	0.79
16	JONSWAP no lab (Phllips 1977)	2.600	1.000	11.18	0.25	0.30	0.54
17	Davidan (1980)	4.363	1.000	16.02	0.28	0.30	0.86
18	Walsh, US coast (1989)	1.860	1.000	14.45	0.29	0.30	0.65
19	Mitsuyasu (1971)	1.600	1.000	21.99	0.33	0.30	0.96
20	JONSWAP (1973)	2.890	1.008	19.72	0.33	0.30	0.97
21	Donelan et al. (1992)	1.700	1.000	22.62	0.33	0.30	1.00
22	Kahma (1986)average. growth	2.000	1.000	22.00	0.33	0.30	1.01
23	Kahma (1981, 1986)rapid. growth	3.600	1.000	20.00	0.33	0.30	1.03

Table 2. Data of numerical experiments

Experiment	p_x	q_x	$10q - 2p$	ε_0	ω_0	$\varepsilon_0^{1/5}\omega_0$
ZRP	1	0.3	1	$2.9 \cdot 10^{-7}$	21.35	1.05
Snyder	0.7	0.23	1	$1.24 \cdot 10^{-5}$	9.04	0.94
Tolman-Chalikov	0.5	0.2	0.9	$3.2 \cdot 10^{-5}$	7.91	1.00
Hsiao-Shemdin	0.5	0.19	0.9	$2.0 \cdot 10^{-5}$	8.16	0.94
Donelan (with dissipation)	0.6	0.21	0.83	$6.1 \cdot 10^{-6}$	10.17	0.92
Donelan (without dissipation)	0.53	0.19	0.84	$2.05 \cdot 10^{-5}$	7.85	0.91
Plant	0.77	0.254	1	$2.9 \cdot 10^{-6}$	12.89	1.006
Stuart-Plant	0.5	0.21	1.1	$1.15 \cdot 10^{-5}$	9.48	0.975

Theory predicts $q_{th} = 0.26$, $s \simeq 1$. These data also support our statement on dominance of the nonlinear resonant process over income from wind. Other experimental and numerical data supporting our theory are collected in article [16]. In field experiments presented in Table 1 the dimensionless fetch χ varies inside the following range: $10^2 < \chi < 10^5$.

We solved the stationary Hasselmann equation (48) numerically, using various models for $\gamma(\omega, \theta)$ (see [18]). The results are presented in the Table 2. The data for the Plant and Stuart-Plant models will be commented on in the paper [41].

In these experiments fetch, χ, varies typically in the limits $0 < \chi < 10^5$. Numerical modeling shows that asymptotically for $\chi > 10^3$ all models of S_{in} lead to formation of powerlike behavior (46) of functions $\tilde{F}(\chi)$ and $\tilde{\sigma}(\chi)$. The prediction of the analytic theory, $10q - 2p = 1$, $s \sim 1$, is satisfied very well. In cases when $\gamma(\sigma)$ is a powerlike function

(ZRP and Plant models), the establishment of powerlike behavior of $\tilde{F}(\chi)$ and $\tilde{\sigma}(\chi)$ occurs for much lower fetches, $\chi \sim 10^2$.

We must stress that in spite of demonstrated universality, different models of wind input lead to completely different predictions on growth of wave energy with fetch. Models of Snyder and Hsiao-Shemdin differ especially dramatically. For all values of fetch $0 < \chi < 10^5$ we have $\tilde{F}_{Snyder}(\chi) > 5\tilde{F}_{Hsiao-Shemdin}(\chi)$

6. Self-similaruty of wind-driven sea

Now we can answer the most "sharpest" questions: Why do both field and laboratory experiments assert that $\tilde{F} = F(\chi)$ and $\sigma = \sigma(\chi)$ are powerlike functions (46)? Why are the exponents p, q are contained inside intervals (47)? We will discuss the Hasselmann sea only, where the Hasselmann equation is applicable.

Let us consider Eq. (48) and assume that $\gamma_{in}(\sigma)$ is a powerlike function

$$\gamma_{in}(\sigma) = \gamma_0 \, \sigma^{1+l} \cdot f(\phi) \tag{52}$$

One can check that Eq. (48) has the following self-similar solution

$$F = \chi^{p+q} \, G(\sigma, \chi, \phi) \tag{53}$$

which leads to powerlike expressions (46) where

$$\epsilon_0 = \int_0^{2\pi} d\phi \int_0^\infty G(\sigma, \phi) \, d\sigma \qquad \omega_0 = \frac{1}{\epsilon_0} \int_0^{2\pi} d\phi \int_0^\infty \sigma G(\sigma, \phi) \, d\sigma \tag{54}$$

In Eq. (53)

$$q = \frac{1}{2+l}, \quad p = \frac{8-l}{2(2+l)} \tag{55}$$

The function $G(\xi, \phi)$, $\xi = \sigma\chi^q$, satisfies the following equation:

$$\cos\phi[(p+q)G + q\xi\frac{\partial G}{\partial \xi}] = \tilde{S}_{nl} + \gamma_0\xi^{1+l} \, f(\phi) \, G \tag{56}$$

Here $\tilde{S}_{nl}$ is a dimensionless S_{nl} and $\gamma_0 \simeq 10^{-5}$ is a dimensionless small parameter. An explicit equation for $\tilde{S}_{nl}$ is presented in [19]. This term can be split into income and outcome terms. Each of them dominates over S_{in}; thus near the spectral peak S_{in} can be neglected and the condition $s = \epsilon^{1/5}\omega_0 \sim 1$ still holds.

Now let us notice that in the ZRP model of S_{in} , $l = 4/3$. This gives $q = 0.3$, $p = 1$, in good accordance with experiments 13-23 presented in Table 1. For the Plant model, $l = 2$; this gives $q = 0.25$, $p = 0.75$, in good accordance with experiments 3-7 in Table 1. In all offered models for S_{in}, $\gamma(\sigma)/\sigma$ is a growing function, and $1 < S < 2.3$. This gives, in virtue of Eq. (55) the following frames for the variation of exponents:

$$0.67 < p < 7/6, \quad 0.22 < q < 0.33$$

These frames are very close to experimentally observed frames (47) and results presented in Table 1. The results of numerical experiments collected in Table 2 show that models of S_{nl} different from the ZRP and Plant models lead to exponents outside the frame (47). This is not a weak point of theory; rather it is a weakness of the discussed models. The major prediction of the theory, the magic relation $10q - 2p = 1$, is satisfied pretty well.

In these models, $\gamma(\sigma)$ are not pure powerlike functions. However S_{in} is still a small term in Eq. (48), and we may seek "quasimodular solutions" such that exponents are "slow functions" of fetch $p = p(\chi)$, $q = q(\chi)$.

Critical analysis of data from field, wave tanks and numerical experiments is summarized in [16], [45]. In these articles the data that cover variation of averaged functions $\tilde{F}(\chi)$ and $\tilde{\sigma}(\chi)$ are collected. In a huge range of fetches, $10 < \chi < 10^6$ the magic relation is valid!

But it doesn't mean that all models for S_{in} are equally good. The analytic model predicts the "magic relation" between p and q as well as a relation between ϵ_0 and ω_0, but it says nothing about absolute values of these quantities. Comparing the first line of Table 1 (Wel et al experiments) with the second line in Table 2 (Snyder model prediction)

we see very good qualitative coincidence but large quantitative differences. The Snyder model overestimates the rate of energy growth with fetch by almost an order of magnitude. Because of the limited length of this article we cannot discuss an extremely important question: the shape of spectra in the universal spectral range $1 < \sigma < 5$. Eq. (48) does not preserve energy that leaks from the Hasselmann sea to the Phillips sea, forming an energy flux P. Thus the solution of Eq. (48) must have asymptotic behavior

$$G(\xi) \to \beta \frac{P^{1/3}}{\sigma^4} \tag{57}$$

Because $\gamma_0 \ll 1$, β is a small number. This implies the inevitable formation of Zakharov-Filonenko spectral tails $F(\omega) \sim 1/\omega^4$. Such tails are routinely observed in numerous field and laboratory experiments, see for example [42], [43]. This important subject deserves a special consideration.

7. Conclusions

Let us summarize the results. We claim that the majority of data obtained in field and numerical experiments can be explained in a framework of a simple model

$$\frac{d\epsilon}{dt} = S_{nl} + \gamma_{in}(\omega, \phi)\epsilon$$

Moreover, most of the facts can be explained by the assumption that $\gamma_{in}(\omega, \phi)$ is a powerlike function on frequency, $\gamma_{in}(\omega, \phi) = \gamma_0 \, \omega^{1+s} \, f(\phi)$. Here $1 < s < 2.3$ and $f(\phi), \gamma_0$ are tunable. This model pertains only to the description of the Hasselmann sea, $0 < \omega < \omega_H$, $\omega_H \simeq (4 - 5)\omega_p$.

In fact, this model is a simplification of the widely accepted model in oceanography (1). What is the difference between these models? The main difference is obvious: we excluded from our consideration any mention of wave energy dissipation. This does not mean that we deny a crucial role of wave-breaking in the dynamics of ocean surface. But, from the spectral viewpoint, the wave-breaking takes place outside the Hasselmann sea. It is going into the Phillips sea, in the spectral area of short scales. This very important statement is supported by experimental data and by numerical solutions of dynamical phase-resolving equations for a free surface.

What we offer could be called "poor man's oceanography." A "poor man" refuses attempts to derive the equation for S_{in} from "first principles," but has in his possession powerful analytic and computer models to use as test beds for compatibility of models for $\gamma_{in}(\omega, \phi)$ with experimental data. The Snyder model does not pass this test and should be excluded from operational models.

Acknowledgements

References

1. O.M. Phillips, On the dynamics of unsteady gravity waves of finite amplitude, Part 1, *J. Fluid Mech.*, 1960; **9** 193-217.
2. K. Hasselmann, On the nonlinear energy transfer in a gravity-wave spectrum. Part 1. General theory.*J. Fluid Mech.*, 1962; **12** 481-500.
3. K. Hasselmann, On the nonlinear transfer in a gravity-wave spectrum. Part II. Conservation theorems; wave-particle analogy; irreversibility. *J. Fluid Mech.*, 1963; **12** 273-281.
4. V.E. Zakharov, N.N. Filonenko, Energy spectrum for stochastic oscillations of the surface of liquid, *Doclady Akad. Nauk SSSR*, 1966; **170(6)** 1292-1295; English:*Sov. Phys. Dokl.*, 1967; **11** 881-884.
5. M.M. Zaslavskii, V.E. Zakharov, The theory of wind wave forecast (in Russian), *Doklady Akad. Nauk SSSR*, 1982; **265 (3)** 567-571.
6. M.M. Zaslavski, V.E. Zakharov, The kinetic equation and Kolmogorov spectra in the weak turbulence theory of wind waves, *Izvestiya Atmospheric and Oceanic Physics*, 1982; **18** 747-753.
7. M.M. Zaslavski, V.E. Zakharov, The shape of the spectrum of energy containing components of the water surface in the weakly turbulent theory of wind waves, *Izvestiya Atmospheric and Oceanic Physics*, 1983; **19** 207-212.
8. S.A. Kitaigorodskii, On the theory of the equilibrium range in the spectrum of wind-generated gravity waves, *J. Phys. Oceanogr.*, 1983; **13** 816-826.

9. V.E. Zakharov, Direct and inverse cascade in wind-driven sea and wave breaking, *Proc. IUTAM Meeting on Wave Breaking, Sydney, 1991*, Eds. M.L. Banner and R.H.Y. Grimshaw, Springer-Verlag, Berlin; 1992, 69-91.

10. V.E. Zakharov, Theoretical interpretation of fetch limited wind-driven sea observations, *Nonlin. Process. Geophys.*, 2005; **12 (6)** 1011-1020.

11. A. Pushkarev, D. Resio, V. Zakharov, Weak turbulent approach to the wind-generated gravity sea waves, *Physica D*, 2003; **184 (1-4)** 29-63).

12. S.I. Badulin, A.N. Pushkarev, D. Resio, V.E. Zakharov, Self-similarity of wind driven seas, *Nonlin. Process. Geophys.*, 2005; **12(6)** 891-945.

13. S.I. Badulin, A.V. Babanin, D. Resio, V.E. Zakharov, Weakly turbulent laws of wind-wave growth, *J. Fluid Mech.*, 2007; **591** 339-378.

14. V.E. Zakharov, Energy balance in a wind-driven sea, *Physica Scripta*, 2010; **T142** 014052.

15. V.E. Zakharov, S.I. Badulin, On energy balance of wind-driven seas, *Doklady Earth Sciences*, 2011; **440(2)** 1440-1444.

16. V. E. Zakharov, S. I. Badulin, Paul A. Hwang, Guillemette Caulliez, Universality of sea wave growth and its physical roots, *J. Fluid Mech.*, 2015; **780** 503-535.

17. V. Zakharov, A. Pushkarev, D. Resio, New wind input term consistent with experimental, theoretical and numerical considerations, *Nonlin. Processes Geophys.*, 2017; **24** 581-597.

18. A. Pushkarev, V. Zakharov, Limited fetch revisited: Comparison of wind input terms, in surface wave modeling, *Ocean Modelling*, 2016; **103** 18-37.

19. V. Geogjaev, V. Zakharov, Numerical and analytical calculations of the parameters of power-law spectra for deep water gravity waves, *JETP Letters*, 2017; **106(3)** 184-187.

20. Cavaleri, L., Alves, J.-H., Ardhuin, F., Babanin, A., Banner, M., Belibassakis, K., Benoit, M., Donelan, M., Groeneweg, J., Herbers, T., Hwang, P., Janssen, P., Janssen, T., Lavrenov, I., Magne, R., Monbaliu, J., Onorato, M., Polnikov, V., Resio, D., Rogers, W., Sheremet, A., I. Smith, J. M., Tolman, H., van Vledder, G., Wolf, J., and Young, I.: Wave modelling The state of the art, Progress in Oceanography, 75, 603 674.

21. Ian R. Young, Wind Generated Ocean Waves, Elsevier, 1999.

22. P. Janssen, The Interaction of Ocean Waves and Wind. Cambridge University Press, 2004.

23. V. Zakharov and A. Pushkarev, Diffusion model of interacting gravity waves on the surface of deep fluid, *Nonlin. Proc. Geophys.*, 1999; **6 (1)** 1-10.

24. V. Geogjaev, V. Zakharov, Self–Similar Swells, (in preparation)

25. V. Zakharov, Statistical theory of gravity and capillary waves on the surface of a finite-depth fluid, *Eur. J. Mech. B/Fluids*, 1999; **18 (3)** 327-344.

26. V. Zakharov, A.O. Korotkevich, A.N. Pushkarev, D. Resio, Coexistence of weak and strong wave turbulence in a swell Propagation, *Phys. Rev. Lett.*, 2007; **99** 164501.

27. A. O. Korotkevich, V. E. Zakharov, Evaluation of a spectral line width for the Phillips spectrum by means of numerical simulation, *Nonlin. Processes Geophys.*, 2015; **22** 325-335.

28. S.Y. Annenkov, V.I. Shrira, Numerical modelling of water-wave evolution based on the Zakharov equation, *J. Fluid Mech.*, 2001; **449** 341-371.

29. S.Y. Annenkov, V.I. Shrira, Direct numerical simulation of downshift and inverse cascade for water wave turbulence, *Phys. Rev. Lett.*, 2006; **96(20)** 204501.

30. A.C. Newell, V.E. Zakharov, Rough sea foam, *Phys. Rev. Lett.*, 1992; **69 (8)** 1149-1151.

31. G.J. Komen, L. Cavaleri, M. Donelan, K. Hasselmann, S. Hasselmann, P.A.E.M. Janssen. Dynamics and Modelling of Ocean Waves. Cambridge University Press (1994)

32. V.E. Zakharov, V.S. L'vov, G. Falkovich, Kolmogorov spectra of turbulence I. Wave turbulence, Springer Series in Nonlinear Dynamics. Berlin: Springer-Verlag. xiii, 264 p. (1992).

33. I. Lavrenov, D. Resio, V. Zakharov, Numerical simulation of weak-turbulent Kolmogorov spectra in water surface waves, Proc. 7th Int. Workshop on Wave Hindcasting and Forecasting, Banff, Alberta, Canada, October 21-25, 2002.

34. L.W. Nordheim, On the kinetic method in the new statistics and its applications in the electron theory of conductivity, *Proc. Roy. Soc. London A*, 1928; **119** 689-698.

35. Y. Lvov, R. Binder, A. Newell, Quantum weak turbulence with applications to semiconductor lasers, *Physica D*, 1998; **121** 317-343.

36. A. Pushkarev, D. Resio, V. Zakharov, Second generation diffusion model of interacting gravity waves on the surface of deep fluid, *Nonlin. Process Geophys.*, 2004; **11 (3)** 329-342.

37. A. Katz, V. Kantorovich, Anisotropic turbulent distribution for waves with a non-decay dispersion laws, *Soviet Physics JETP*, 1974; **38** 102-107.

38. W. Pierson, L. Moscowitz, A proposed spectral form for fully developed wind seas based on the similarity theory, *J. Geophys. Res.*, 1964; **69** 5181-5190.

39. W.J. Plant, A relationship between wind stress and wave slope, *J. Geophys. Res.*, 1982; **87 (C3)** 1961-1967.

40. S.A. Kitaigorodskii, On the equilibrium ranges in wind-wave dynamics and ratio probing of the ocean surface, Ed. by O.M. Phyllips and K. Hasselmann. Plenum Press Corp. 9-40, 1986.

41. A. Pushkarev, Comparison of different models for wave generation of the Hasselmann equation (to be published).

42. Y. Toba, Local balance in the air-sea boundary processes. III. On the spectrum of wind waves, *J. Oceanogr. Soc. Japan*, 1973; **29** 209-220.

43. O. Phillips, Spectral and statistical properties of the equilibrium range in wind-generated gravity waves, *J. Fluid Mech.*, 1985; **156** 505-561.

44. S. Badulin, V. Zakharov, Ocean swell within the kinetic equation for water waves, *Nonlin. Processes Geophys.*, 2017; **24** 237253.

45. E. Gagnaire-Renou, M. Benoit, S. Badulin, On weakly turbulent scaling of wind sea in simulations of fetch-limited growth, *J. Fluid Mech.*, 2011; **669** 178213.